

# METHODS FOR BUNCH SHAPE MONITOR PHASE RESOLUTION IMPROVEMENT

A. Feschenko, S. Gavrilov<sup>†</sup>

Institute for Nuclear Research of the Russian Academy of Sciences, Moscow, Russia

## Abstract

Bunch shape monitors, based on secondary electron emission, are widely used for measurements of longitudinal bunch profiles during linac commissioning and initial optimization of beam dynamics. The typical phase resolution of these devices is about 1°. However it becomes insufficient for new modern linacs, which require a better resolution. Some methods developed for a phase resolution improvement are discussed.

## INTRODUCTION

The technique of a coherent transformation of a temporal bunch structure into a spatial charge distribution of low energy secondary electrons through RF-modulation was initially implemented by R. Witkover [1] for BNL linac. An energy (longitudinal) RF-modulation of secondary electrons was used. In the Bunch Shape Monitor (BSM) [2], developed in INR RAS, a transverse RF-scanning is used. The general principle of BSM operation has been described elsewhere and is clear from Fig. 1.

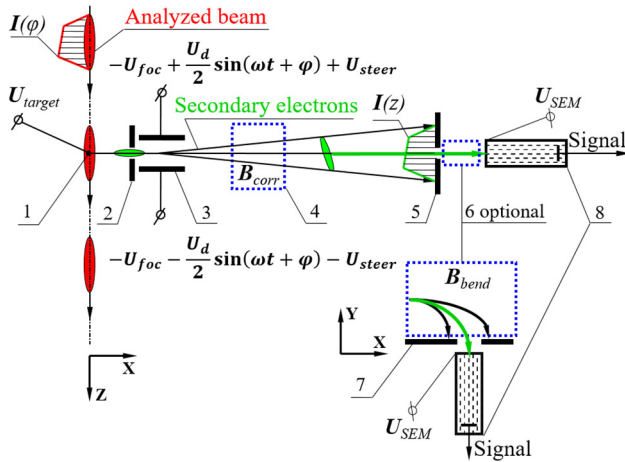


Figure 1: BSM scheme: 1 – tungsten wire target, 2 – inlet collimator, 3 – RF-deflector combined with electrostatic lens, 4 – correcting magnet, 5 – outlet collimator, 6 – optional bending magnet, 7 – registration collimator, 8 – secondary electron multiplier.

Secondary electrons are scanned by a deflecting RF-field and their position  $Z$  depends on its phase and amplitude:

$$Z = Z_0 + Z_{max} \sin \varphi. \quad (1)$$

BSM resolution can be defined as a full width at a half maximum of a spread function for infinitely short bunches. Due to a finite phase resolution the measured distribution is smoothed and a fine bunch structure can be lost.

<sup>†</sup> s.gavrilov@gmail.com

By differentiation of Eq. (1) the phase resolution can be written as:  $\Delta\varphi = \Delta Z / (Z_{max} \cos\varphi)$ , assuming, that  $\Delta Z$  is a FWHM size of the electron beam. Substituting  $\varphi$  from Eq. (1) one can write the phase resolution for the coordinate of the outlet collimator  $Z = Z_c$  as:

$$\Delta\varphi = \frac{\Delta Z}{Z_{max} \sqrt{1 - \frac{(Z_c - Z_0)^2}{Z_{max}^2}}}. \quad (2)$$

Evidently, the phase resolution can be improved, if the steering voltage  $U_{steer}$  is adjusted to direct the electrons into the outlet collimator, when the deflecting RF-field is off. In this case  $Z_c = Z_0$ , and the resolution equals:

$$\Delta\varphi = \frac{\Delta Z}{Z_{max}}. \quad (3)$$

The value of a maximum deflection  $Z_{max}$  can be found from electrical and mechanical parameters of the detector, so the main problem is to estimate accurately the size  $\Delta Z$  of the electron beam and to propose ways for its decreasing. Sometimes instead of FWHM  $\Delta Z$  it is more convenient to use the double RMS size  $2\sigma_z$ .

Modern ion linacs under construction, such as FRIB MSU or ESS ERIC are foreseen to operate with RMS bunch lengths of about 10÷20 ps at medium energies and even shorter at high energies, and at least 0.5° phase resolution is required for reliable bunch shape diagnostics in these linacs.

## RF & STATIC ELECTRIC FIELDS

The main unit of BSM is RF-deflector. The deflector is combined with the electrostatic lens thus enabling simultaneous focusing and RF-scanning of the electrons. Typically, BSM deflectors are RF-cavities, based on parallel wire lines with capacitive plates. An electrical length of the deflectors is usually  $\lambda/4$  or  $\lambda/2$ .

To improve the uniformity of both deflecting and focusing fields in Y-direction, thus improving a phase resolution, the new  $\lambda$ -type symmetric cavity has been developed for BSM-ESS (Fig. 2).

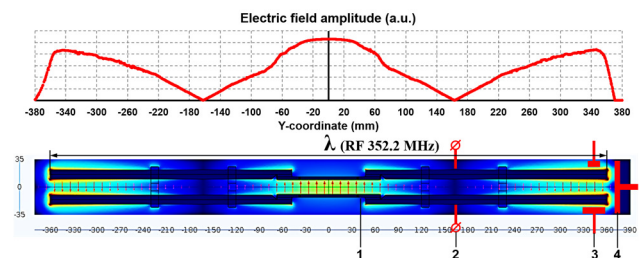


Figure 2: E-field distribution in  $\lambda$ -type deflector.

The electrodes with deflecting plates 1 are supported by ceramic insulators. Focusing potentials are applied to the electrodes through spring contacts 2 at zero field points. Capacitive adjustable couplers 3 are used to drive the cavity and to pick up the RF-signal. The fine tuning of the resonant frequency is provided with capacitive tuner 4 via the manual actuator from outside the vacuum.

Figure 3 shows the distribution of the RF-field  $E_z$ -component in YZ-plane ( $X = 0$ ) in the non-symmetric ( $\lambda/2$ ) and the symmetric ( $\lambda$ ) deflectors. The uniformity of the field in a zone of the electron beam passage is an order of magnitude better for the symmetric type.

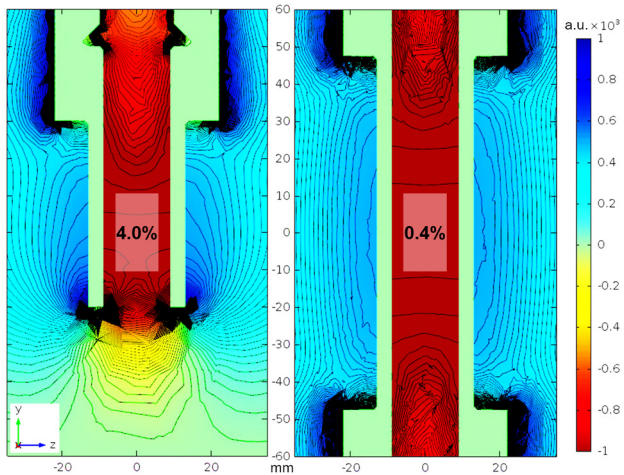


Figure 3: RF-field  $E_z$ -component distribution in YZ-plane ( $X = 0$ ) of  $\lambda/2$ - and  $\lambda$ -type BSM deflectors.

The length of the deflecting plates in X direction is optimized to get the maximum deflection amplitude  $Z_{max}$  for the selected BSM geometry and the target potential. For example, for BSM-ESS  $Z_{max} = 68$  mm for  $U_{target} = -10$  kV and  $U_d = 1$  kV.

The electrostatic lens focuses the electron beam to completely fit into the outlet collimator (typically 0.5 mm width and 10 mm length). Figure 4 shows the e-beams at the outlet collimator for three  $\delta$ -function analyzed bunches with the interval of  $0.5^\circ$  (352.2 MHz).

In these simulations the initial energy of the electrons corresponded to the typical energy distribution function of secondary electrons [3] and initial angles with respect to emitting surface were supposed to be distributed uniformly within the hemisphere.

The double RMS size of the focused beams in Fig. 4 equals  $2\sigma_z = 0.25$  mm, so in principle the size of the slit can be decreased to 0.25 mm with the aim to improve the resolution to  $\Delta\phi_0 = 57.3 \cdot 0.25 / 68 = 0.21^\circ$ . However it should not be done due to two reasons.

The first reason is decreasing of intensity of the detected electron beam. The second one is presence of one more crucial component of the phase resolution not yet discussed – time dispersion (delay) of secondary electron emission. The value of the delay time is not known exactly. The theoretical value for metals is estimated to be about 0.01 ps [3]. The experimental attempts to measure the time dispersion give the upper limit of this value equal to  $(4 \pm 2)$  ps [4] rather than a real one.

3 Technology

3G Beam Diagnostics

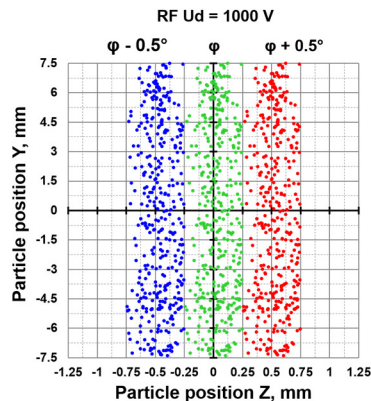


Figure 4: Transverse cross-sections of the e-beam in the plane of the outlet collimator for different phases of deflecting field.

We assume the delay time of the emission to be uniformly distributed within the range of  $0 \div 6$  ps, so the double RMS delay equals 3.46 ps, which is equivalent to  $\Delta\phi_{SEE} = 0.44^\circ$  for 352.2 MHz. The resulting phase resolution can be found as  $\sqrt{(\Delta\phi_0)^2 + (\Delta\phi_{SEE})^2} = 0.48^\circ$ , thus the corresponding slit for 68 mm amplitude of RF-scan is 0.57 mm.

MAGNETIC FIELDS

A proper focusing can be provided for non-distorted electron beam only, which is hardly achievable in practice due to the presence of external fringe magnetic fields. The distortions of electron trajectories in Z-direction are compensated by adjusting the steering voltage  $U_{steer}$ . To compensate the distortions in other directions the correcting static magnetic fields are used.

Correcting Magnet

The correcting magnet with the combination of dipole and quadrupole fields (Fig. 5a) is implemented. The dipole field produced with two coils moves the electron beam along Y-axis. The quadrupole field produced with another four coils enables to adjust the tilt of the beam image in YZ-plane (Fig. 5b).

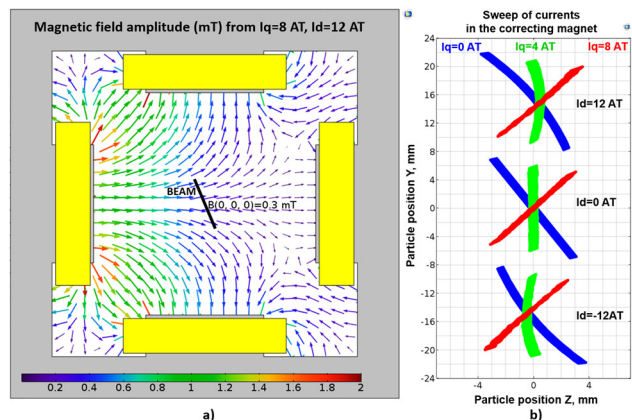


Figure 5: (a) Superposition of dipole and quadrupole fields of the correcting magnet. (b) Cross-sections of the e-beam in the plane of the outlet collimator for different quadrupole  $I_q$  and dipole  $I_d$  coil currents (Ampere·Turns).

The three corrections provide an exhaustive fit of the electron beam and the outlet collimator, thus compensating an influence of external moderate static magnetic fields. But sometimes BSMs are installed in a close vicinity of magnetic focusing elements (quads and correctors) with strong fringe fields. Besides, alternating magnetic fields which cannot be corrected with the above described technique fundamentally are present. In this case magnetic shields of different configurations can be used.

### Magnetic Shield

Typical BSM shield represents a sectional jacket made of 2 mm low-carbon steel with relative permeability  $\mu_r \sim 500$ . Additionally, the interior surfaces can be covered with a foil made of an amorphous cobalt-iron alloy with high  $\mu_r$ . Figure 6 shows the effect of the BSM shield on the fringe field of the quad located in the vicinity of BSM. Red line represents the component  $B_Y$  without and green one with the shield. The analysis has shown that the distortions of the electron trajectories arising due to the remnant fringe fields can be compensated with the described corrections.

Even better results (blue curves) can be obtained if additional 2 mm low-carbon steel plate screens are added upstream and downstream of BSM. The remnant fields decrease to the level less, than the Earth's magnetic field, and their influence on electron trajectories will be definitely negligible.

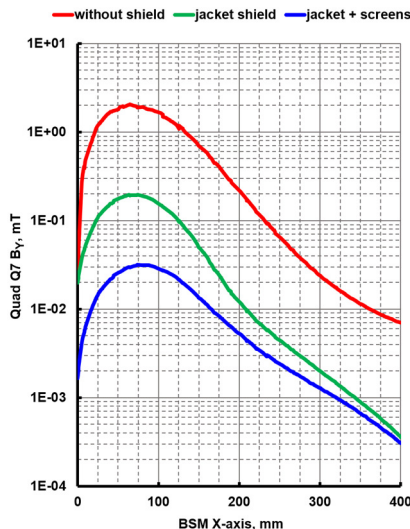


Figure 6: Quad  $B_Y$  distribution along BSM X-axis.

Of course, the shield influence on the lattice of the accelerator focusing system is to be checked.

### BEAM SPACE CHARGE

All estimations described above are done with the assumption of a zero-intensity analysed beam, while a space charge of the real beam can strongly influence the secondary electrons trajectories and result in phase resolution deterioration.

The methods of taking into account the space charge of the analyzed beam are described in [5]. As an example, the results of simulations for ESS proton linac at different beam currents are presented in Fig. 7.

ISBN 978-3-95450-169-4

The phase resolution is given as a function of a longitudinal coordinate along the bunch. The bunch head is at the left side in the figure.

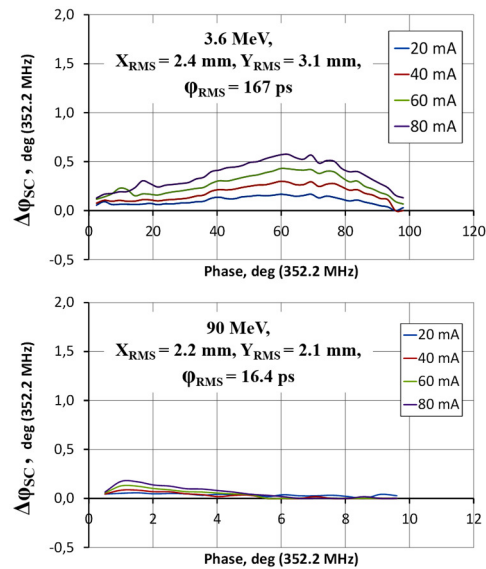


Figure 7: Space charge effect for various beam currents.

Also the energy modulation of secondary electrons by the space charge can result in a phase reading error, when the measured phase coordinate along the bunch does not correspond to the real one.

### CONCLUSION

Bunch Shape Monitor is a reliable tool for longitudinal beam studies. A variety of measures have been developed and implemented lately to improve BSM phase resolution: the new  $\lambda$ -type symmetric RF-deflector for uniformity of the deflecting and focusing fields, special magnetic shield for protection against external fringe magnetic fields and correcting magnet with the combination of dipole and quadrupole fields for compensation of remnant magnetostatic fields and misalignments of BSM elements.

All these improvements enable to achieve  $0.5^\circ$  phase resolution for hundreds of MHz for zero beam intensity which corresponds to about 4 ps and is determined mainly by the time dispersion of the secondary electron emission. Space charge effects do not increase it crucially even in case of high-intensity beams of forthcoming ion linacs.

### REFERENCES

- [1] R. Witkover, "A non-destructive bunch length monitor for a proton linear accelerator", *Nucl. Instr. Meth.*, vol. 137, no. 2, pp. 203-211, 1976.
- [2] A. Feschenko, "Technique and instrumentation for bunch shape measurements", in *Proc. RUPAC2012*, Saint-Petersburg, Russia, Oct. 2012, pp. 181-185.
- [3] I. M. Bronstein, B. S. Fraiman, Secondary electron emission. Moscow, Russia: Nauka, 1969 (in Russian).
- [4] E. Ernst, H. Von Foerster, "Time dispersion of secondary electron emission", *J. of Appl. Phys.*, vol. 26, no. 6, pp. 781-782, 1955.
- [5] A. Feschenko, V. Moiseev, "Peculiarities of bunch shape measurements of high intensity ion beams", in *Proc. IPAC-10*, 2010, pp. 1065-1067.